ISBN: 978-3-95450-248-6 ISSN: 2673-5490 doi: 10.18429/JACoW-IPAC2025-WEAD2

HIGH POWER RF TESTING OF HIGH TEMPERATURE SUPERCONDUCTORS

A. Dhar*, M. E. Schneider, G. P. Le Sage, E. A. Nanni,
SLAC National Accelerator Laboratory, Menlo Park,California,USA
J. Golm, P. Krkotić, W. Wuensch, S. Calatroni, CERN, Geneva, Switzerland
J. Gutierrez , ICMAB-CSIC, Barcelona, Spain

Abstract

Superconducting materials such as niobium have been extremely useful for accelerator technology but require low temperature operation 2 K. The development of high temperature superconductors (HTS) is promising due to their operating temperatures being closer to that of liquid nitrogen 77 K. This work aims to determine the high-power RF performance of these materials at X-band (11.424 GHz). We have tested several types of rare earth barium copper oxide (REBCO) materials, such as films deposited by electron-beam physical vapor deposition, coated conductors soldered to a copper substrate, and solid pucks formed from powder. RF testing was done via a hemispherical TE mode cavity that maximizes the magnetic field and minimizes the electric field on a 2-inch sample region. We will report on surface resistance vs temperature measurements at high power,as well as RF testing of a pulse compression cavity lined with REBCO coated conductors.

INTRODUCTION

Superconducting rf (SRF) materials such as niobium (Nb) have been extremely useful for improving rf cavity efficiency but require extremely low temperatures for operation ~ 2-4 K [1–3]. Niobium cavities at 1.3 GHz have been able to reach quality factors over 10^{10}, as compared to room temperature normal conducting rf (NCRF) cavities which typically reach quality factors of 10^4 – 10^5 at the same frequency [2].

The development of high temperature superconductors (HTS) is promising due to their significantly higher transition temperatures. Rare earth barium copper oxides (REBCO) are particularly interesting because their critical temperature of approximately ~90 K. Furthermore, REBCO is commercially available as coated conductors (CC) and in constant development in form of other coatings, making it suitable for resonant structures. HTS cavities could be cooled by liquid nitrogen instead of liquid helium, drastically reducing the cryogenic infrastructure required for operation. Structures coated with HTS materials could be used as high Q devices such as linearizers, deflector cells, axion cavities, and pulse compressors [4–6].

A key drawback of using any superconductor are limitations on the induced surface magnetic field, which can cause the structure to rapidly transition. This normally limits the gradient of niobium structures to gradients on the order of 50 MV/m [7]. This is about five times less than their NCRF cavities, which can operate at gradients up to 250 MV/m [8]. Thus it is vital to understand the transition dynamics of REBCO in order to benchmark them against niobium for use in SRF cavities.

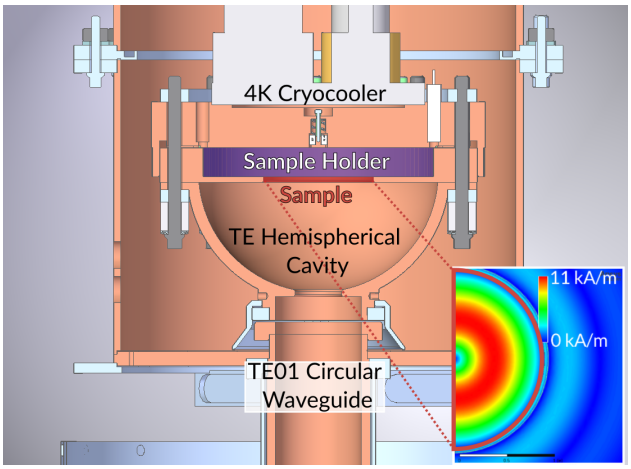

Figure 1: Cross-sectional view of the hemispherical cavity within the cryostat. The sample holder (purple) allows for 2 inch samples (red) to be easily swapped out for rf measurements. The fields on the sample (insert) have azimuthal symmetry due to the TE023 mode within the cavity. Fields are shown for 1.6 kW of input power.

EXPERIMENTAL SETUP

Two distinct classes of REBCO samples with different coating techniques and surface treatments were tested, coated conductor tape samples and vapor deposited film samples. For further details on these samples please refer to our previous proceedings [9]. These samples were tested at varying power levels within a hemispherical cavity designed to have a TE_{023} mode at 11.424 GHz [10]. This mode minimizes the electric field on the sample surface and maximizes the magnetic field. We can model these fields with high precision by using ANSYS HFSS simulation tools, and even determine the rf response in frequency space. This allowed us to properly conduct steady-state measurements of the SRF characteristics when applying low power (<1 mW).

At higher power (>1 kW), the cavity is used for time domain measurements of superconducting transition dynamics for a given surface magnetic field. The hemispherical cavity is coupled into a TE_{01} circular waveguide that can be connected to either a vector network analyzer (VNA) or an X-

* adhar@slac.stanford.edu

ISBN: 978-3-95450-248-6 ISSN: 2673-5490 doi: 10.18429/JACoW-IPAC2025-WEAD2

band traveling wave tube (TWT) that can provide up 1.6 kW pulses over 8 µs. The VNA by comparison provides less than 1 mW to the cavity. A schematic of the hemispherical cavity installed in the experimental cryostat can be seen in Fig. 1. The base of the cavity is designed to allow for 2 inch samples to be easily swapped out for rf measurements [10].

HIGH POWER TESTING

With the steady-state performance well characterized, the next step was to measure transition dynamics by applying stronger surface fields to the sample. These measurements were performed from 100 W to 1.6 kW of input rf power, which can provide 2 to 11 kA/m surface magnetic field. Each pulse was 8 µs long, with a repetition rate of 100 Hz. Forward power was ramped up at each temperature setpoint, in order to better ascertain the relationship between sample conductivity and applied surface field near the transition point. Figure 2 shows an example of reflected power measurement from the cavity. The exponential decay during the rf pulse represents the state of the cavity as it fills with rf energy, while the decay after the pulse represents the state of cavity afterwards.

This second decay was fit to an exponential function, with a time constant τ that is inversely proportional to the total quality factor of the cavity based on $Q_t = -\pi f_0/\tau$, where f_0 is the resonant frequency of the cavity in MHz. Prior analysis of the steady-state data determined that the external quality factor (Q_e) was roughly constant over the temperature range of interest (4 K to 100 K). This meant that Q_0 could be determined from the following equation:

$$\frac{1}{Q_0} = \frac{1}{Q_t} - \frac{1}{Q_e}. \tag{1}$$

Thus with this internal quality factor we can extract the contribution of the sample and in turn its conductivity based on the following:

$$\frac{1}{Q_0} = \frac{1}{Q_s} + \frac{1}{Q_{cav}} \tag{2}$$

$$\sigma_s = \sigma_{ref}\left(\frac{Q_s}{Q_{s,ref}}\right)^2. \tag{3}$$

The sample quality factor (Q_s) can be obtained from the internal quality factor (Q_0), which is a combination of Q_s and the quality factor of the cavity itself (Q_{cav}). From here, the rf conductivity of the sample (σ_s) is determined by using a reference conductivity for bulk Cu σ_{ref} and then measuring a reference $Q_{s,ref}$ for the cavity with a bulk Cu sample in it. The reference conductivity for copper is 58 MS/m, which would give a $Q_{s,ref}$ of 1.5×10^5 [11]. These values would be used to extract the conductivity of the sample as a function of temperature and applied power.

These results are summarized in Fig. 3. While the film sample was able to reach a higher conductivity that is closer to the ideal value, it also was more drastically affected by applied fields and began transitioning closer to 86 K instead

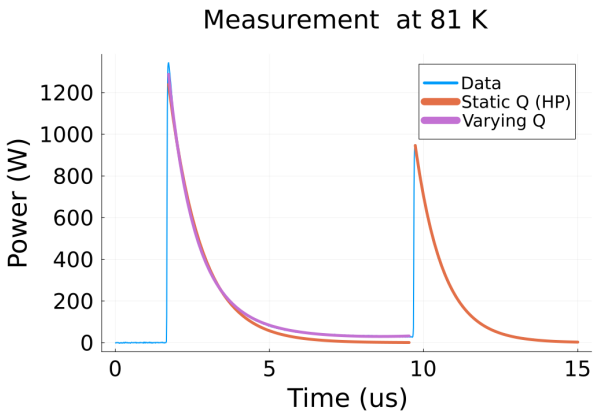

Figure 2: Plot of reflected power (blue) from cavity at 81 K for 1600 kW input power. At this power level, the assumption that the quality factor is constant during the rf pulse (orange) does not fit this decay accurately.

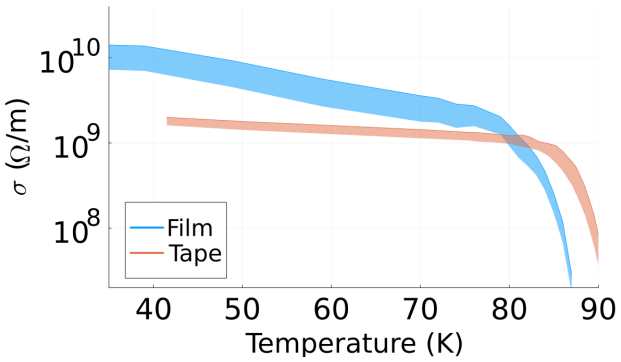

Figure 3: Plots of conductivity for both REBCO samples at the end of the rf pulse, with the shaded regions representing the range of values as a function of forward power, between 100 W (upper limit) and 1600 W (lower limit).

of the expected critical temperature of 89 K. However in order to properly understand the transition dynamics for these samples, we would need to study in more detail how quickly these transitions occur within the rf pulse.

Looking at the decay in reflected power during the rf pulse, initial attempts at fitting the data to a constant quality factor were not successful, as shown in Fig. 2. To correct for this, a time-varying model of the internal quality factor was used to correctly fit the data [12]. This revealed that the initial quality factor was close to the steady-state values, before rapidly dropping over several microseconds, as shown in Fig. 4. Comparing the effective conductivity of the sample during the pulse to the steady-state measurements of the sample allows us to infer how much of the sample transitions during the pulse, shown in Fig. 4b. At most about 70% of the sample has transitioned once the cavity fields saturate, implying that effective heating induced by these fields is not enough to warm the entire sample past the critical point.

To better map out where these points of near total transition are, the decay in reflected power during the pulse was

ISBN: 978-3-95450-248-6 ISSN: 2673-5490 doi: 10.18429/JACoW-IPAC2025-WEAD2

(a)

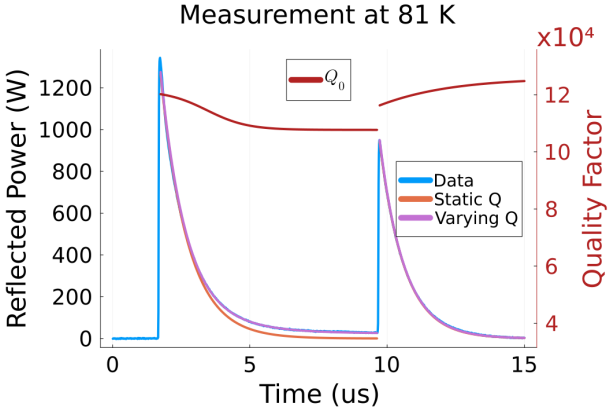

(b)

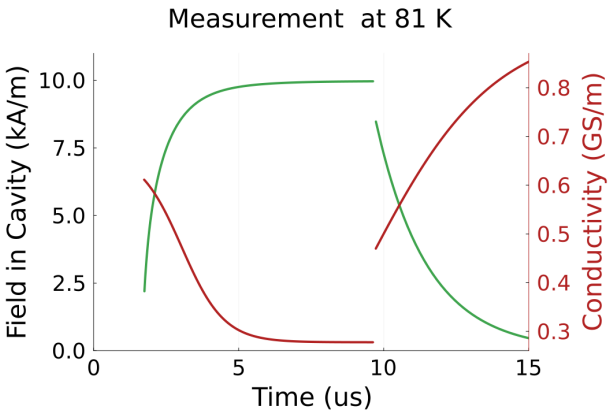

Figure 4: (a) Plot of reflected power (blue) from cavity at 81 K for 1600 kW input power. At this power level, the assumption that the quality factor is constant (orange) does not fit this decay accurately. However if a time-varying Q model is used (purple), the data can be fit correctly, extracting Q_0 as a function of time (red). Once the rf power is turned off, the quality factor quickly slowly with time as power dissipates within the cavity. (b) Based on the characteristics of the cavity, the applied field to the sample can also be extracted (red), allowing us to estimate the conductivity of the sample as a function of time (red).

compared to an exponential fit assuming a fixed time constant. Based on the χ^2 value of this fit exceeding a certain threshold, the surface fields and temperatures corresponding to the onset of the transition boundary can be identified, as shown in Fig. 5. As with Fig. 3 above, the deposited film sample begins to transition at a slightly lower temperature as compared to the tape sample, but the overall slope is similar for both samples. This suggests that the relation between surface magnetic field and critical temperature is approximately linear. This would mean that the trend in critical point is due to the HTS reaching a critical current boundary, as opposed to a critical temperature boundary which would scale with the square of the applied field [13].

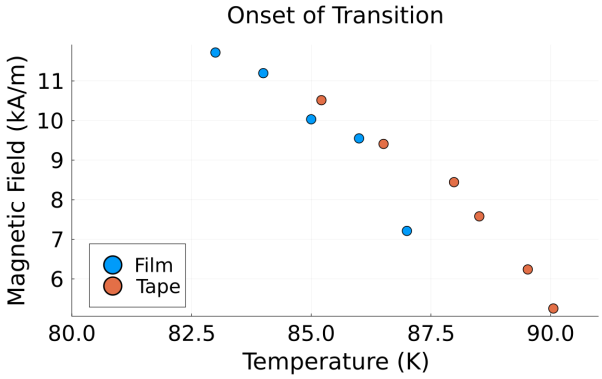

Figure 5: Plot of the points where a near total transition during the pulse occurs, with the film sample (blue) starting to transition at slightly lower temperatures than the tapes sample (orange). Both of these trends are roughly linear, but more data at higher field strength will clarify this.

Based on pulsed surface heating models, we expect the average temperature rise within the sample to be no more than 0.1 K [14]. This does not account for any hot spots that may occur from gaps, surface impurities, or areas of bad electrical or thermal conductivity [15]. Furthermore, since we can determine that the conductivity of the sample saturates as the cavity fields saturate, any effective heating induced by these fields is not enough to warm the entire sample by the requisite amounts for a transition.

Thus far we have tested these materials up to 11 kA/m peak surface magnetic field, which would generate an accelerating gradient of roughly 3 MV/m in a standard SRF cavity [2]. Understanding these limits and mechanisms behind them will be the subject of future study as we prepare to test these samples with up to 2 MW of rf power in order to observe transitions at lower temperatures. These studies will be crucial to determining the utility of HTS cavities made from REBCO materials for high power rf applications.

ACKNOWLEDGMENTS

The authors would like to thank Valery Borzenets, Matt Boyce, Paul Welander, and Sami Tantawi for many helpful discussions. This work is supported by U.S. Department of Energy Contract No. DE-AC02-76SF00515.

REFERENCES

[1] D. Gonnella *et al.*, "Nitrogen-doped 9-cell cavity performance in a test cryomodule for LCLS-IIa)", *J. Appl. Phys.*, vol. 117, no. 2, p. 023908, Jan. 2015. doi:10.1063/1.4905681

[2] B. Aune *et al.*, "Superconducting TESLA cavities", *Phys. Rev. ST Accel. Beams*, vol. 3, no. 9, p. 092001, Sep. 2000. doi:10.1103/PhysRevSTAB.3.092001

[3] A. Brachmann, M. Dunham, and JF. Schmerge, "LCLS-II - Status and Upgrades", in *Proc. FEL'19*, Hamburg, Germany, Aug. 2019, pp. 772–775. doi:10.18429/JACoW-FEL2019-FRA02

ISBN: 978-3-95450-248-6 ISSN: 2673-5490 doi: 10.18429/JACoW-IPAC2025-WEAD2

[4] J. Golm *et al.*, "Thin Film (High Temperature) Superconducting Radiofrequency Cavities for the Search of Axion Dark Matter", *IEEE Trans. Appl. Supercond.*, vol. 32, no. 4, pp. 1–5, 2022. doi:10.1109/TASC.2022.3147741

[5] A. Miyazaki, "Potential of Nonconventional Superconductors for Particle Accelerator Cavities", *IEEE Trans. Appl. Supercond.*, vol. 34, no. 7, pp. 1–6, 2024. doi:10.1109/TASC.2024.3430067

[6] S. Ahyoune *et al.*, "RADES axion search results with a high-temperature superconducting cavity in an 11.7 T magnet", *J. High Energy Phys.*, vol. 2025, Apr. 2025. doi:10.1007/JHEP04(2025)113

[7] D. Bafia, A. Grassellino, OS. Melnychuk, AS. Romanenko, Z.-H. Sung, and J. Zasadzinski, "Gradients of 50 MV/m in TESLA Shaped Cavities via Modified Low Temperature Bake", in *Proc. SRF'19*, Dresden, Germany, Aug. 2019, pp. 586–591. doi:10.18429/JACoW-SRF2019-TUP061

[8] V. Dolgashev, S. Tantawi, Y. Higashi, and B. Spataro, "Geometric dependence of radio-frequency breakdown in normal conducting accelerating structures", *Appl. Phys. Lett.*, vol. 97, no. 17, p. 171501, 2010. doi:10.1063/1.3505339

[9] A. Dhar *et al.*, "REBCO sample testing at high power X-band", in *Proc. IPAC'24*, Nashville, TN, USA, May 2024, pp. 2772–2774. doi:10.18429/JACoW-IPAC2024-WEPS37

[10] PB. Welander, MA. Franzi, and SG. Tantawi, "Cryogenic RF Characterization of Superconducting Materials at SLAC With Hemispherical Cavities", in *Proc. SRF'15*, Whistler, BC, Canada, Sep. 2015, pp. 735–738. doi:10.18429/JACoW-SRF2015-TUPB065

[11] N. J. Simon *et al.*, *Properties of copper and copper alloys at cryogenic temperatures. Final report*. NIST, 1992. doi:10.6028/NIST.MONO.177

[12] A. Cahill, JB. Rosenzweig, V. Dolgashev, z. Li, S. Tantawi, and S. Weathersby, "RF losses in a high gradient cryogenic copper cavity", *Phys. Rev. Accel. Beams*, vol. 21, Jun. 2018. doi:10.1103/PhysRevAccelBeams.21.061301

[13] T. Junginger, W. Weingarten, and C. Welsch, "RF characterization of superconducting samples", in *Proc. SRF'09*, Berlin, Germany, Sep. 2009, paper TUOBAU03, pp. 130–134. https://accelconf.web.cern.ch/SRF2009/papers/tuobau03.pdf

[14] D. P. Pritzkau and R. H. Siemann, "Experimental study of RF pulsed heating on oxygen free electronic copper", *Phys. Rev. ST Accel. Beams*, vol. 5, no. 11, p. 112002, Nov. 2002. doi:10.1103/PhysRevSTAB.5.112002

[15] G. Hampel *et al.*, "High power failure of superconducting microwave filters: investigation by means of thermal imaging", *Appl. Phys. Lett.*, vol. 69, no. 4, pp. 571–573, Jul. 1996. doi:10.1063/1.117790